© 2014. Published by The Company of Biologists Ltd | Development (2014) 141, 1209-1221 doi:10.1242/dev.101014

RESEARCH ARTICLE

STEM CELLS AND REGENERATION

Distinct Wnt-driven primitive streak-like populations reflect *in vivo* lineage precursors

Anestis Tsakiridis*, Yali Huang, Guillaume Blin, Stavroula Skylaki, Filip Wymeersch, Rodrigo Osorno, Costas Economou, Eleni Karagianni, Suling Zhao, Sally Lowell and Valerie Wilson*

ABSTRACT

During gastrulation, epiblast cells are pluripotent and their fate is thought to be constrained principally by their position. Cell fate is progressively restricted by localised signalling cues from areas including the primitive streak. However, it is unknown whether this restriction accompanies, at the individual cell level, a reduction in potency. Investigation of these early transition events *in vitro* is possible via the use of epiblast stem cells (EpiSCs), self-renewing pluripotent cell lines equivalent to the postimplantation epiblast. Strikingly, mouse EpiSCs express gastrulation stage regional markers in self-renewing conditions. Here, we examined the differentiation potential of cells expressing such lineage markers. We show that undifferentiated EpiSC cultures contain a major subfraction of cells with reversible early primitive streak characteristics, which is mutually exclusive to a neural-like fraction. Using *in vitro* differentiation assays and embryo grafting we demonstrate that primitive streak-like EpiSCs are biased towards mesoderm and endoderm fates while retaining pluripotency. The acquisition of primitive streak characteristics by self-renewing EpiSCs is mediated by endogenous Wnt signalling. Elevation of Wnt activity promotes restriction towards primitive streak-associated lineages with mesendodermal and neuromesodermal characteristics. Collectively, our data suggest that EpiSC pluripotency encompasses a range of reversible lineage-biased states reflecting the birth of pioneer lineage precursors from a pool of uncommitted EpiSCs similar to the earliest cell fate restriction events taking place in the gastrula stage epiblast.

KEY WORDS: Epiblast stem cells, Gastrulation, Heterogeneity, Neuromesodermal progenitors, Primitive Streak, Wnt signalling, Mouse

INTRODUCTION

Lineage specification in the mouse embryo during gastrulation generates progressively more restricted precursors from initially uncommitted postimplantation epiblast cells (Tzouanacou et al., 2009). Cell fate restriction is spatially organised (Lawson et al., 1991) by localised signalling cues and is reflected by the regionalised expression of lineage-specific markers (Pfister et al., 2007; Arnold and Robertson, 2009; Teo et al., 2011). However, pluripotency is widespread in the epiblast until around the start of somitogenesis (Osorno et al., 2012). A defining feature of gastrulation is the formation of the primitive streak (PS), a posterior structure in which epiblast cells undergo epithelial-to-mesenchymal (EMT) transition, ingressing to give rise initially to the endoderm and mesoderm of the head and heart, and later to progressively more posterior mesoderm types, including somites (Kinder et al., 1999; Kinder et al., 2001). Anterior epiblast that does not encounter the PS instead forms ectoderm-restricted lineages, including the anterior neural ectoderm (Lawson, 1999; Cajal et al., 2012). Clonal analysis showed that some early-ingressing mesodermal derivatives arise from a common mesendodermal (ME) precursor, whereas later-ingressing somitic mesoderm is generated by a neuromesodermal (NM) progenitor, which also gives rise to the neurectoderm of the spinal cord (Tzouanacou et al., 2009).

One of the earliest markers for the PS is the T-box transcription factor *T*(*Bra*), which is expressed both in pre-EMT prospective mesoderm and endoderm in the posterior epiblast, and in post-EMT, nascent mesoderm in the PS and its descendant, the tail bud (Wilkinson et al., 1990; Kispert and Herrmann, 1994; Rivera-Pérez and Magnuson, 2005; Burtscher and Lickert, 2009). *T*(*Bra*) is also expressed in the node and notochord. Wnt and Nodal signalling are essential for both PS specification (Liu et al., 1999; Ben-Haim et al., 2006) and the initiation of T(Bra) expression (Conlon et al., 1994; Arnold et al., 2000).

Despite considerable progress in defining the role of the interactions between signalling pathways and regionalised genetic activity in the induction of PS precursors, the inaccessibility of mouse embryos renders the study of the transition from pluripotency to lineage restriction difficult. Epiblast stem cells (EpiSCs), cell lines derived from the postimplantation epiblast (Brons et al., 2007; Tesar et al., 2007) or from embryonic stem cells (ESCs) *in vitro* (Guo et al., 2009), represent an attractive model for dissecting early lineage commitment as they comprise the *in vitro* counterpart of pluripotent cells in the gastrula stage epiblast (Huang et al., 2012). Unlike mouse ESCs but similar to human ES cells (hESCs), self-renewal of EpiSCs, reflected by the simultaneous expression of the key pluripotency factors *Oct4* (*Pou5f1* – Mouse Genome Informatics), *Nanog* and *Sox2*, relies on culture in the mesoderm inducers Activin (inhibin – Mouse Genome Informatics), a Nodal-like TGFβ family member, and Fgf2 (Tesar et al., 2007; Vallier et al., 2009; Greber et al., 2010). Like the gastrulating epiblast (Pfister et al., 2007; Arnold and Robertson, 2009), EpiSC lines also express, under self-renewing conditions, lineage-specific markers (Tesar et al., 2007; Bernemann et al., 2011; Teo et al., 2011; Iwafuchi-Doi et al., 2012; Kojima et al., 2014). Variations in their expression at the population level have been shown to result in altered differentiation outcome (Bernemann et al., 2011). However, whether heterogeneous lineage-specific marker expression is an inherent feature of EpiSC pluripotency, reflecting the emergence

MRC Centre for Regenerative Medicine, Institute for Stem Cell Research, School of Biological Sciences, University of Edinburgh, 5 Little France Drive, Edinburgh EH16 4UU, UK.

*Authors for correspondence (a.tsakiridis@ed.ac.uk; v.wilson@ed.ac.uk)

Received 29 July 2013; Accepted 6 January 2014

Development (2014) doi:10.1242/dev.101014

of pioneer lineage-biased yet uncommitted precursors, or a manifestation of commitment to specific lineages induced by culture conditions is presently unknown.

Here we dissect the events underlying the progressive commitment of pluripotent EpiSCs to PS-derived lineages. Using a T(Bra)-based, PS-specific fluorescent reporter, we characterise a major self-renewing fraction of undifferentiated EpiSCs that exhibits early gastrulation, pre-ingression (i.e. epiblast-like) PS characteristics and readily interconverts with reporter-negative cells. PS-like EpiSCs are dependent on endogenous Wnt signalling and are biased towards mesodermal and endodermal differentiation with retention of pluripotency. Further elevation of Wnt activity drives cells out of pluripotency, producing two mutually exclusive cell types resembling ME and NM progenitors present in the PS *in vivo*. Collectively, our findings suggest that, *in vivo*, regional gene expression defines cells in the gastrulation stage epiblast that are biased towards, but not committed to, distinct differentiation outcomes.

RESULTS

Two major subpopulations in EpiSC cultures reflecting PS and neurectoderm

Previous studies have reported the expression of lineage-specific markers in self-renewing EpiSC populations (Tesar et al., 2007; Bernemann et al., 2011; Kojima et al., 2014). We sought to extend these findings at the single cell level. Immunocytochemistry revealed that the early PS marker T(Bra) (Rivera-Perez and Magnuson, 2005) is expressed heterogeneously in undifferentiated EpiSCs irrespective of whether they were derived from ESCs *in vitro* or from the postimplantation epiblast (Fig. 1A; supplementary material Fig. S1). Image analysis showed that many T(Bra)$^+$ cells co-expressed the main pluripotency markers: epiblast-specific Oct4 and Nanog, and epiblast/neural marker Sox2 (Fig. 1A; supplementary material Fig. S1). We also observed some colocalisation between Nanog and the endoderm/organiser/axial mesoderm marker Foxa2 (Sasaki and Hogan, 1993) (supplementary material Fig. S1A). Collectively, these data indicate that EpiSCs, marked by Oct4, Nanog and Sox2 expression, heterogeneously express PS markers, suggesting that PS-like subpopulations are not products of spontaneous differentiation.

To further characterise EpiSC heterogeneity, we established a PS reporter EpiSC line (Tps/tb-RED), which showed a characteristic EpiSC expression profile and dependence on Activin signalling (supplementary material Fig. S2). We used a dsRed2 transgene under the transcriptional control of a randomly integrated *T*(*Bra*) promoter fragment (Tps/tb) shown to be active specifically in the PS and the tail bud but not the notochord (Clements et al., 1996; Yamaguchi et al., 1999). Analysis of E8.5 chimeric embryos following blastocyst injection of Tps/tb-RED ESCs confirmed dsRed2 expression specifically in the PS and nascent paraxial mesoderm (supplementary material Fig. S2). Furthermore, Tps/tb promoter activity was already detectable by the onset of gastrulation in the PS of E6.5 chimeras (supplementary material Fig. S3).

In EpiSC conditions, we found that a prominent fraction of Tps/tb-RED EpiSCs (15-30%) expressed dsRed2 (Fig. 1B). Quantitative PCR (qPCR) analysis of flow cytometry-sorted dsRed2$^+$ and dsRed2$^-$ EpiSC populations revealed that dsRed2$^+$ cells were enriched for early PS and organiser markers (Fig. 1C), whereas expression of neural-related genes was more pronounced in the dsRed2$^-$ fraction (Fig. 1C). Expression of late PS markers, activated at the end of gastrulation (*Wnt3a*, *Cdx4* and *Nkx1-2*) (Gamer and Wright, 1993; Takada et al., 1994; Schubert et al., 1995), as well as the differentiated somitic mesoderm marker *Meox1* (Candia et al., 1992) was low in both populations (Fig. 1C). At the protein level, dsRed2 positivity predominantly marked T(Bra)$^+$ cells that were either Foxa2$^+$ or Foxa2$^-$ (Fig. 1D). By contrast, most dsRed2$^-$ cells were negative for both T(Bra) and Foxa2, although about 20% expressed Foxa2 but not T(Bra) (Fig. 1D). Only a few dsRed2$^+$ cells co-expressed the neural markers nestin (Nes) (Lendahl et al., 1990) and Cdh2 (Radice et al., 1997) (Fig. 1E,F). Taken together, these data suggest that under conditions promoting an undifferentiated state, heterogeneous expression of the Tps/tb promoter-driven dsRed2 reporter marks an EpiSC fraction enriched in early PS-like cells.

The depletion of neural markers in dsRed2$^+$ cells prompted us to investigate whether the dsRed2$^-$ population includes neural-like cells. To this end, an EpiSC line was established from 46C ESCs that carry a GFP reporter within the neurectoderm-specific *Sox1* locus (Wood and Episkopou, 1999; Ying et al., 2003). Analysis of Sox1-GFP EpiSCs by flow cytometry showed that ~20-25% of cells were GFP$^+$ (Fig. 1G). These were found by immunostaining to express very low or no T(Bra) protein (Fig. 1G). Flow sorted Sox1-GFP$^+$ cells were significantly enriched for neural-specific transcripts such as *Sox1* itself and, to a lesser extent, *Pax6* (Grindley et al., 1995) (Fig. 1H) while expressing lower levels of early PS markers than their negative counterparts (Fig. 1H), in line with the observation that PS-like, Tps/tb-dsRed2$^+$ EpiSCs express low levels of neural markers (Fig. 1C,E,F). Thus, undifferentiated EpiSCs are significantly heterogeneous and contain at least two major mutually exclusive subpopulations characterised by the expression of early PS and neural markers, respectively.

PS-like EpiSCs are self-renewing EpiSCs

We next asked whether dsRed2$^+$, PS and Sox1-GFP$^+$, neural-like EpiSCs are capable of self-renewal. Like T(Bra)$^+$ cells (Fig. 1A; supplementary material Fig. S1) most dsRed2$^+$ EpiSCs expressed the pluripotency markers Oct4, Nanog and Sox2 (Fig. 2A). Moreover, they were positive for Cdh1, which marks early epithelia, including the postimplantation epiblast and endoderm. As T(bra) is not expressed in the endoderm (Burtscher and Lickert, 2009), this suggests that Tps/tb-dsRed2 expression characterises pre-ingression, epiblast cells rather than committed, post-EMT mesoderm (Fig. 2B). This suggests that PS-like EpiSCs are undifferentiated cells. We therefore tested whether dsRed2$^+$ and dsRed2$^-$ cells can self-renew. We flow sorted the two populations and re-plated them in EpiSC conditions. The resulting cultures arising from both dsRed2$^+$ and dsRed2$^-$ cells exhibited characteristic EpiSC colony morphology and Oct4 expression (Fig. 2E). Moreover, daily fluorescence-activated cell sorting (FACS) analysis showed that by day 5 both sorted populations had re-equilibrated the routinely observed percentage of dsRed2$^+$ cells (compare Fig. 2C with Fig. 1B). The two sorted populations expanded at a comparable rate, excluding the possibility of the apparent interconversion of dsRed$^+$ and negative cells occurring by selective growth of one population over the other (Fig. 2D). Thus, the PS-like EpiSC subpopulation exists in dynamic equilibrium with dsRed2$^-$ cells, and both fractions exhibit features of undifferentiated EpiSCs.

To further verify the link between PS character and capacity for self-renewal, we sorted dsRed2$^+$ and dsRed2$^-$ cells, re-plated them at clonal density and examined by immunofluorescence the presence of T(Bra)$^+$ cells in the resulting clones after culture in EpiSC conditions. Both populations generated clones containing T(Bra)$^+$ cells although dsRed2$^+$ derived clones contained a slightly higher proportion of T(Bra)$^+$ cells (Fig. 2F). Most clones comprised either

Development (2014) doi:10.1242/dev.101014

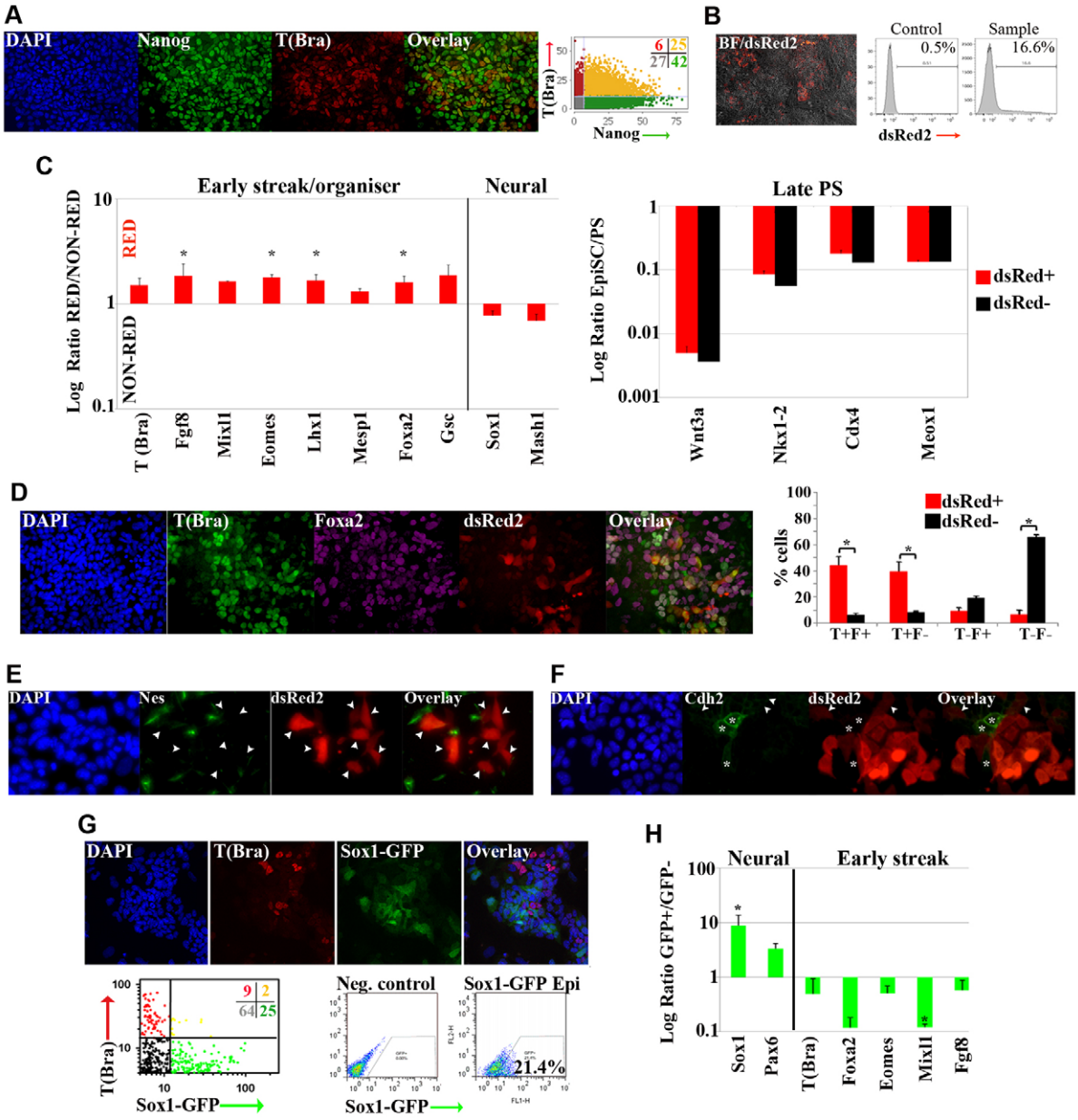

Fig. 1. Undifferentiated EpiSCs contain two major subpopulations. (A) Nanog and T(Bra) immunocytochemistry in undifferentiated, wild-type EpiSCs. Graph: immunofluorescence quantitation following single cell image analysis. Numbers: percentages of cells in each quadrant. (B) dsRed2 expression in undifferentiated Tps/tb-RED EpiSCs assessed by fluorescence microscopy (left) and flow cytometry (right). (C) qPCR for indicated markers in sorted dsRed2^{+} and dsRed2^{-} Tps/tb-RED EpiSCs. Results are represented as $\log_{10}$ ratio of expression versus dsRed2^{-} cells (left) (*P<0.05, Student's t-test) or dissected E8.5 PS (right). Error bars: s.e.m. (n=3). (D) Left, fluorescence analysis of dsRed2, T(Bra) and Foxa2 expression in Tps/tb-RED EpiSCs. Right, quantitation of T(Bra) and Foxa2 positivity in dsRed2^{+} and dsRed2^{-} populations after immunostaining of Tps/tb-RED EpiSCs and image analysis. T, T(Bra); F, Foxa2. Error bars: s.e.m. (n=3), *P<0.05 (chi-squared test). (E) Nes immunocytochemistry and dsRed2 fluorescence. Arrowheads: dsRed2^{+} cells. (F) Cdh2 immunocytochemistry and dsRed2 fluorescence. Asterisks, Cdh2^{high} cells; arrowheads, dsRed2^{+}/Cdh2^{low} cells. (G) Top: GFP and T(Bra) immunocytochemistry in Sox1-GFP EpiSCs. Bottom left: quantification of T(Bra) and Sox1-GFP expression domains. Bottom right: fluorescence-activated cell sorting (FACS) analysis of GFP expression in self-renewing Sox1-GFP EpiSC cultures. (H) qPCR analysis of neural and early PS marker expression in sorted Sox1-GFP^{+} and Sox1-GFP^{-} EpiSCs. Results are represented as log (GFP^{+}/GFP^{-} cell) values. Error bars: s.e.m. (n=3), *P<0.05 (Student's t-test). BF, Brightfield.

T(Bra)$^{+}$ or T(Bra)$^{-}$ cells. However, some were heterogeneous, containing both T(Bra)$^{+}$ and T(Bra)$^{-}$ cells (24/127 from dsRed^{+} and 16/136 from dsRed^{-}, of which a total of 20 contained ≤4 cells). This indicates that interconversion occurs not only between dsRed2 reporter positive and negative cells, but also between T(Bra)$^{+}$ and T(Bra)$^{-}$ states, which can interconvert within one to two divisions. (Fig. 2F). These results additionally suggest that the PS characteristics we observed in EpiSCs do not compromise clonogenicity in culture conditions promoting an undifferentiated state.

We next examined whether neural-like Sox1-GFP^{+} EpiSCs also exhibit features of undifferentiated, self-renewing cells. In contrast to dsRed2^{+} cells, which were predominantly positive for the main three pluripotency factors, only about half of Sox1-GFP^{+} EpiSCs co-expressed Oct4 and Nanog, suggesting that the rest of the GFP^{+} cells had undergone neural commitment (supplementary material Fig.

Development (2014) doi:10.1242/dev.101014

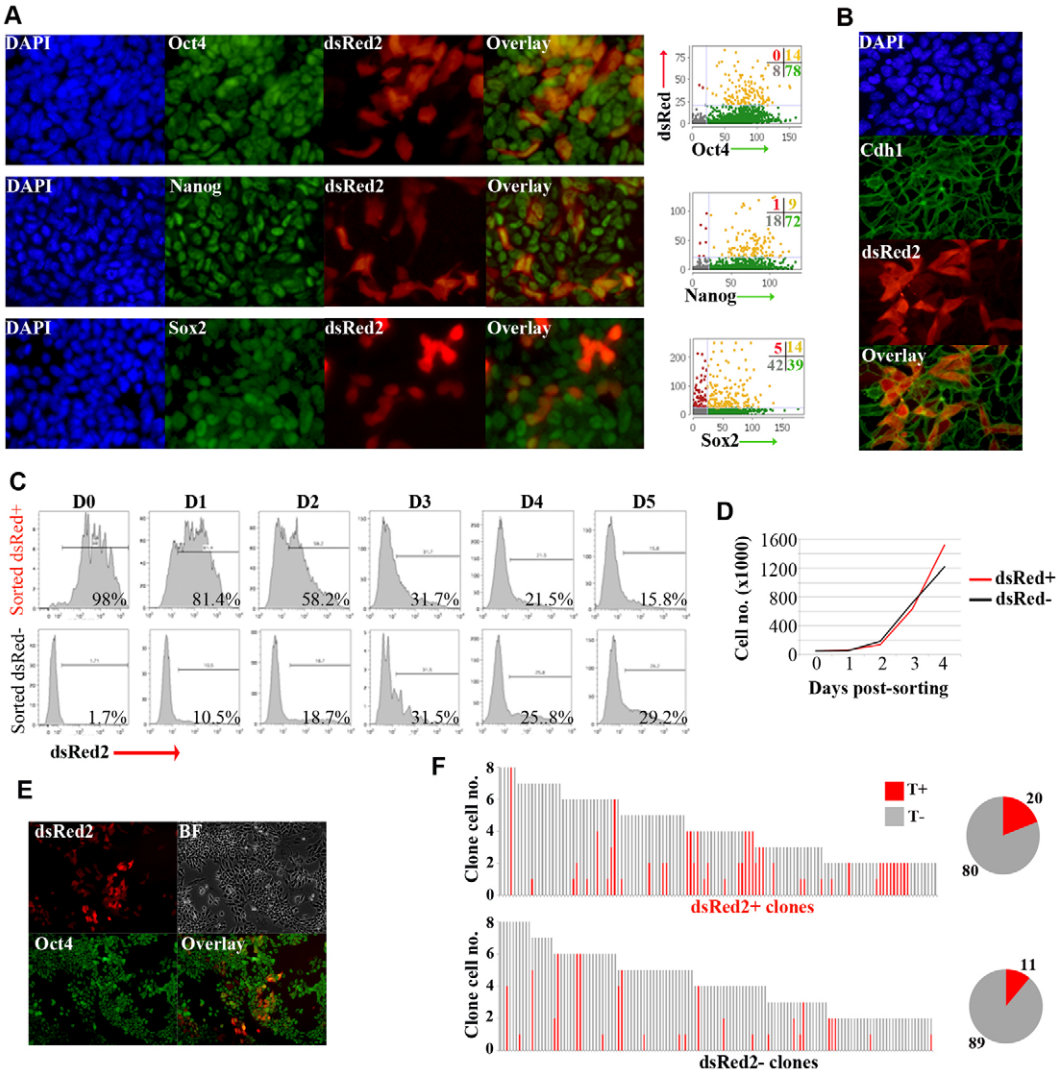

Fig. 2. PS-like Tps/tb-RED EpiSCs comprise a dynamic undifferentiated and self-renewing subpopulation. (A) Oct4, Nanog and Sox2 immunocytochemistry. Right, image analysis of dsRed2 and indicated pluripotency markers (B) Cdh1 immunocytochemistry and dsRed2 fluorescence. (C) Flow cytometry-based timecourse analysis of dsRed2 expression in sorted and replated dsRed^{+} and dsRed^{-} populations in EpiSC conditions. (D) Numbers of sorted dsRed2^{+} and dsRed2^{-} cells post-sorting. (E) Oct4 immunocytochemistry and dsRed2 fluorescence at day 6 post-sorting of dsRed2^{-} cells. (F) Composition of colonies obtained after plating sorted dsRed2^{+} and dsRed2^{-} EpiSC at clonal density for 72 hours and immunohistochemistry for T(Bra) expression. Each bar in the *x*-axis represents a single clone. *y*-axis: number of T(Bra)$^{+}$ (red) or T(Bra)$^{-}$ (grey) cells/clone. Number of clones: $N_{dsRed+clones}$=127, $N_{dsRed-clones}$=136. Pie charts: overall percentages of cells of either phenotype (number of cells: $N_{dsRed+cells}$=534, $N_{dsRed-cells}$=584).

S4A). When sorted Sox1-GFP^{+} and negative cells were re-plated in EpiSC conditions, the two fractions showed a degree of interconversion, although the ability of Sox1-GFP^{-} EpiSCs to regenerate the GFP^{+} subpopulation was limited (supplementary material Fig. S4B). Taken together, the above data show that PS-like, Tps/tb-dsRed2^{+} EpiSCs exhibit hallmark features of bona fide undifferentiated EpiSCs such as expression of pluripotency factors and self-renewal ability. By contrast, Sox1-GFP^{+} neural-like EpiSC subpopulations are less dynamic and may contain cells committed to neural differentiation, consistent with the observation that *Sox1* mRNA levels are upregulated in EpiSC derivatives during neural differentiation (Iwafuchi-Doi et al., 2012).

Wnt signalling induces PS identity in undifferentiated EpiSCs

Two candidate signals could, in theory, directly induce dsRed2 expression: Wnt and Activin/Nodal (Latinkić et al., 1997; Yamaguchi et al., 1999; Lee et al., 2011). As Activin is essential for EpiSC self-renewal and thus Activin/Nodal signalling should be active in both dsRed2– and dsRed2+ populations, we hypothesised that localised endogenous Wnt signalling drives dsRed2 expression. We observed that dsRed2+ EpiSCs were modestly enriched, and Sox1-GFP^{+} EpiSCs were slightly depleted, for the β-catenin target *Axin2* (supplementary material Fig. S5A). This suggests that PS-like EpiSCs experience higher levels of Wnt activity than their negative counterparts. We therefore tested whether Wnt signalling generates and/or maintains Tps/tb-RED EpiSCs.

Flow cytometry analysis showed that treatment of Tps/tb-RED EpiSCs with the Wnt ligand inhibitor Wif1 (Hsieh et al., 1999) significantly reduced the percentage of dsRed2^{+}-expressing cells (Fig. 3A). Wnt signalling attenuation resulting from the treatment was supported by a decrease in the mRNA levels of the Wnt targets *T*(*Bra*) and *Axin2* (Fig. 3E), a reduction in the protein levels of T(Bra) (Fig. 3B), and the expression of other early streak markers

Development (2014) doi:10.1242/dev.101014

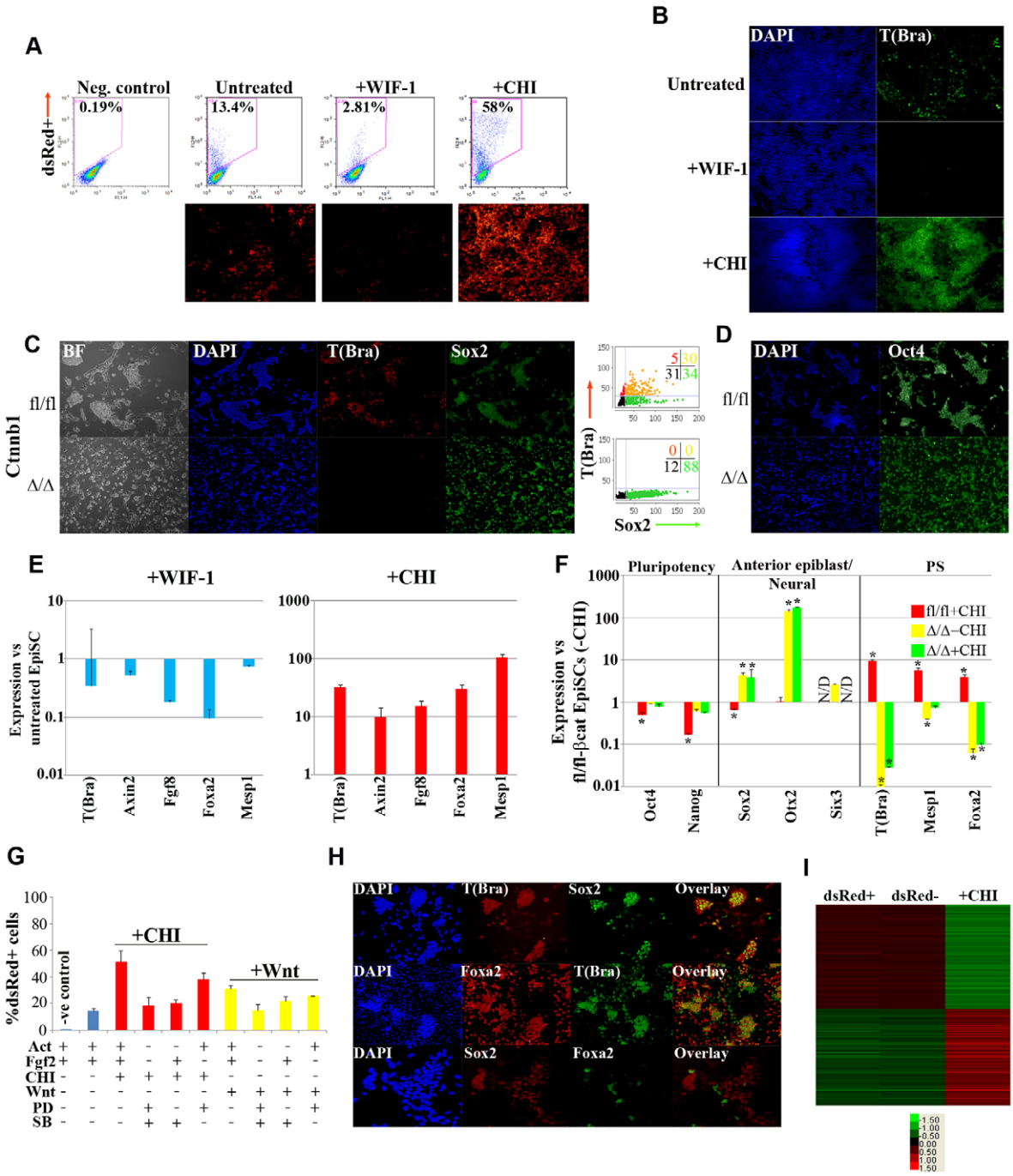

Fig. 3. Wnt signalling confers PS characteristics upon EpiSCs. (A) FACS analysis (upper row) and dsRed2 fluorescence (lower row) of dsRed2-expressing cells in untreated Tps/tb-RED EpiSC cultures and after treatment with Wif1 (120 hours) or CHIRON99021 (CHI) (48 hours) in Activin/Fgf2. (B) Immunocytochemistry of T(Bra) expression in control untreated, Wif1- and CHI-treated Tps/tb-RED EpiSCs. (C,D) T(Bra), Sox2 (C) and Oct4 (D) immunocytochemistry in fl/fl– and Δ/Δ-β-cat EpiSCs. Graphs: image analysis of T(Bra) and Sox2 immunofluorescence. (E) qPCR analysis of indicated markers in untreated, Wif1- (left) and CHI-treated (right) Tps/tb-RED EpiSCs. Expression is represented as $\log_{10}$ ratio versus untreated control. Error bars: s.d. (n=2) for +Wif1 and s.e.m. (n=3) for +CHI (P<0.05 for all genes shown relative to untreated EpiSCs, Student's t-test). (F) qPCR analysis of indicated markers in fl/fl– and Δ/Δ-β-cat EpiSCs in self-renewing conditions and after 48 hours of CHI treatment. Expression is depicted as $\log_{10}$ ratio versus fl/fl EpiSCs (–CHI). Error bars: s.e.m. (n=3). N/D, not determined. *P<0.05, compared with fl/fl– β-cat EpiSCs (–CHI). (G) Percentage of dsRed2-positive cells determined by flow cytometry after 48-hour inhibitor/cytokine treatment of Tps/tb-RED EpiSC. Error bars represent s.d. (n=2). (H) Immunocytochemistry of T(Bra), Sox2 and Foxa2 in CHI-treated EpiSC cultures. (I) Heatmap representing all differentially expressed genes (≥1.5-fold change) between sorted dsRed2 positive and negative fractions and CHI-treated EpiSCs. SB, SB431542; PD, PD0325901; Wnt, Wnt3a.

(Fig. 3E; supplementary material Fig. S5B). Thus, Tps/tb-dsRed2 expression in undifferentiated EpiSCs depends on extracellular Wnt signalling. Interestingly, 5-day treatment with Wif1 had no obvious effect on either undifferentiated cell morphology (data not shown) or the expression of pluripotency factors *Oct4*, *Nanog* and *Sox2* (supplementary material Fig. S5B).

To determine whether Tps/tb-dsRed2 expression was dependent on canonical [β-catenin (*Ctnnb1*)-mediated] Wnt signalling, we

Development (2014) doi:10.1242/dev.101014

established an EpiSC line from floxed β-catenin ESCs (fl/fl-β-cat) (Brault et al., 2001) also carrying a CreER^{T2} cassette knocked into the ROSA26 locus (supplementary material Fig. S6A-C). 4-Hydroxytamoxifen-induced deletion of both floxed *Ctnnb1* alleles did not adversely affect the growth, self-renewal (Fig. 3C) or Activin dependence (supplementary material Fig. S6D) of the resulting β-cat-null (Δ/Δ) EpiSC line, although β-cat Δ/Δ EpiSCs formed smaller colonies, possibly reflecting the role of *Ctnnb1* in cell adhesion (Lyashenko et al., 2011). Thus Wnt/β-catenin signalling is not an essential mediator either of self-renewal or the Activin response. Consistent with the hypothesis that the effects of Wnt inhibition by Wif1 are primarily mediated through β-catenin, T(Bra) expression was completely ablated, and other PS markers strongly downregulated, in *Ctnnb1* null EpiSCs (Fig. 3C,F). By contrast, control fl/fl-β-cat EpiSCs, like Tps/tb-RED EpiSCs, exhibited heterogeneous T(Bra) expression (Fig. 3C,F). However, probably because of the more severe effects of deleting a unique effector of Wnt signalling compared with addition of an inhibitor protein, β-cat Δ/Δ EpiSCs also exhibited a striking upregulation of *Sox2*, *Otx2* and, to a lesser extent, *Six3*, which are expressed by the anterior epiblast undergoing neural specification (Iwafuchi-Doi et al., 2012; Acampora et al., 2013; Cajal et al., 2012) (Fig. 3C,F). By contrast, levels of the pluripotency factors *Oct4* and *Nanog* were unchanged (Fig. 3D,F). Collectively, the above results indicate that Wnt/β-catenin signalling is pivotal for inducing the PS-like EpiSC state at the expense of an anterior epiblast-like fraction, but is dispensable for EpiSC maintenance.

Elevation of Wnt signalling activity promotes distinct precursor-like populations

We next assessed the effects of elevating Wnt signalling levels in EpiSCs. Short-term treatment of EpiSCs with CHIRON99021 (CHI), a potent Gsk-3 (Gsk3b – Mouse Genome Informatics) inhibitor that stabilises β-catenin and activates Wnt targets (Ring et al., 2003; Murray et al., 2004), in EpiSC conditions greatly enhanced both dsRed2 and T(Bra) protein expression (Fig. 3A,B,E). Treatment of cultures with recombinant Wnt3a protein also led to a more modest increase in the number of Tps/tb-dsRed2$^+$ cells (Fig. 3G). Interestingly, the Alk4/5/7 (Acvr1b/Tfgbr1/Acvr1c – Mouse Genome Informatics) Activin/Nodal receptor inhibitor SB431542 (SB43) (Inman et al., 2002) negated the CHI or Wnt3a-driven increase in dsRed2$^+$ cell numbers, whereas MEK inhibition with PD0325901 had a less prominent effect (Fig. 3G). This suggests that full Wnt stimulation of Tps/tb promoter transcription requires active Nodal/Activin signalling.

The increase in Tps/tb-dsRed2 expression after CHI treatment of EpiSC cultures was accompanied by a significant upregulation of both Wnt-responsive genes and other PS-specific markers (Fig. 3E; supplementary material Fig. S5B) as well as a decrease in the expression of pluripotency factors (supplementary material Fig. S5C). Interestingly, although CHI treatment of *Ctnnb1*-null EpiSCs did not alter their undifferentiated, anterior epiblast-like phenotype, it induced a small but significant (P<0.05, Student's t-test) upregulation of *T*(*Bra*) and *Mesp1* relative to untreated Ctnnb1-null cells (Fig. 3F). This indicates that the control of PS identity is not exclusively β-catenin-dependent. Furthermore, CHI treatment of Sox1-GFP EpiSCs considerably reduced the GFP-expressing fraction (supplementary material Fig. S5D). Interestingly, the remaining Sox2$^+$ cells that persisted in the CHI-treated cultures were predominantly T(Bra)$^+$ (Fig. 3H). These T(Bra)$^+$Sox2$^+$ cells were generally mutually exclusive to a Foxa2$^+$ fraction, part of which also co-expressed T(Bra) (Fig. 3H). This suggests that Wnt stimulation promotes the generation of both T(Bra)$^+$Foxa2$^+$ and T(Bra)$^+$Sox2$^+$ cells. Double positivity for T(Bra) and Foxa2 has been linked to a common ME precursor (Kubo et al., 2004; Gadue et al., 2006). Furthermore, in several vertebrates, T(Bra)/Sox2 co-expression marks a region containing NM axial progenitors (Martin and Kimelman, 2012; Olivera-Martinez et al., 2012). We previously showed that, in the early somite stage mouse embryo, NM progenitors reside in the node-streak border (NSB) and the region lateral to the PS (Cambray and Wilson, 2007). We confirmed that cells in this region also co-expressed T(Bra) and Sox2 in the mouse (supplementary material Fig. S7). Thus CHI treatment of EpiSCs mediates the production of two mutually exclusive populations exhibiting features of distinct progenitors: ME precursors marked by T(Bra)/Foxa2 co-expression and T(Bra)$^+$Sox2$^+$ NM progenitors.

Microarray expression profiling of CHI-treated EpiSCs showed that elevation of Wnt signalling induced dramatic global changes in the EpiSC transcriptome (2815 differentially expressed genes based on a 1.5-fold change threshold with FDR ≤0.05) (Fig. 3I). Inspection of the reported expression patterns of the most upregulated transcripts confirmed that CHI treatment significantly induced genes representative of PS-derived lineages and Wnt-related transcripts (supplementary material Table S1). We also noted upregulation of Hox transcripts predominantly belonging to paralogous groups 5-9, which are activated during late gastrulation (reviewed in Deschamps et al., 1999) (supplementary material Fig. S5E). By contrast, two of the most downregulated genes after CHI treatment were the pluripotency factors *Oct4* and *Nanog* (supplementary material Table S1). Interestingly, CHI addition also considerably reduced the levels of anterior neural markers such as *Pou3f1* and *Zic2* (Iwafuchi-Doi et al., 2012) (supplementary material Table S1; data not shown) while posterior neural plate-specific transcripts such as *Zic3* and *Gbx2* (Iwafuchi-Doi et al., 2012) were upregulated (supplementary material Table S1; data not shown). Collectively, the above findings indicate that CHI-mediated elevation of Wnt activity promotes exit from pluripotency, suppresses anterior neural cell fate and drives PS-like cell differentiation towards derivatives produced *in vivo* by distinct ME and NM precursor populations.

PS-like EpiSCs exhibit increased mesendodermal differentiation *in vitro*

Regionalised expression of T(Bra) and Wnt3 within the postimplantation embryo has been shown to precede the differentiation of pluripotent epiblast cells to PS-associated lineages (Rivera-Pérez and Magnuson, 2005; Burtscher and Lickert, 2009). We therefore tested whether the Wnt-dependent dsRed$^+$ PS-like cells are functionally distinct from their dsRed$^-$ counterparts. We first tested the ability of the dsRed2$^+$ and dsRed2$^-$ populations to generate distinct lineage derivatives using embryoid body-like aggregate (EB) formation (Tesar et al., 2007). We FACS-sorted dsRed2$^+$ and dsRed2$^-$ EpiSCs and, after generating EBs from each fraction, we quantified the emergence of beating cardiomyocytes during differentiation (Fig. 4A). EBs derived from the PS-like EpiSC fraction contained a higher proportion of both beating foci and cells positive for the early cardiac transcription factor Nkx2-5 (Searcy et al., 1998) than dsRed2$^-$-derived EBs (Fig. 4A,B).

We also assessed the induction of cardiac (*Mesp1*), cardiac/gut endoderm (*Gata4*, *Gata6*) (Morrisey et al., 1996; Saga et al., 1999) and paraxial/somitic mesoderm (*Meox1*, *Hoxb1*, *Tbx6*) (Candia et al., 1992; Chapman et al., 1996; Forlani et al., 2003) markers by qPCR in EBs differentiated for 3 days after sorting dsRed2$^+$ and dsRed2$^-$ EpiSCs. We found that expression of several of these

Development (2014) doi:10.1242/dev.101014

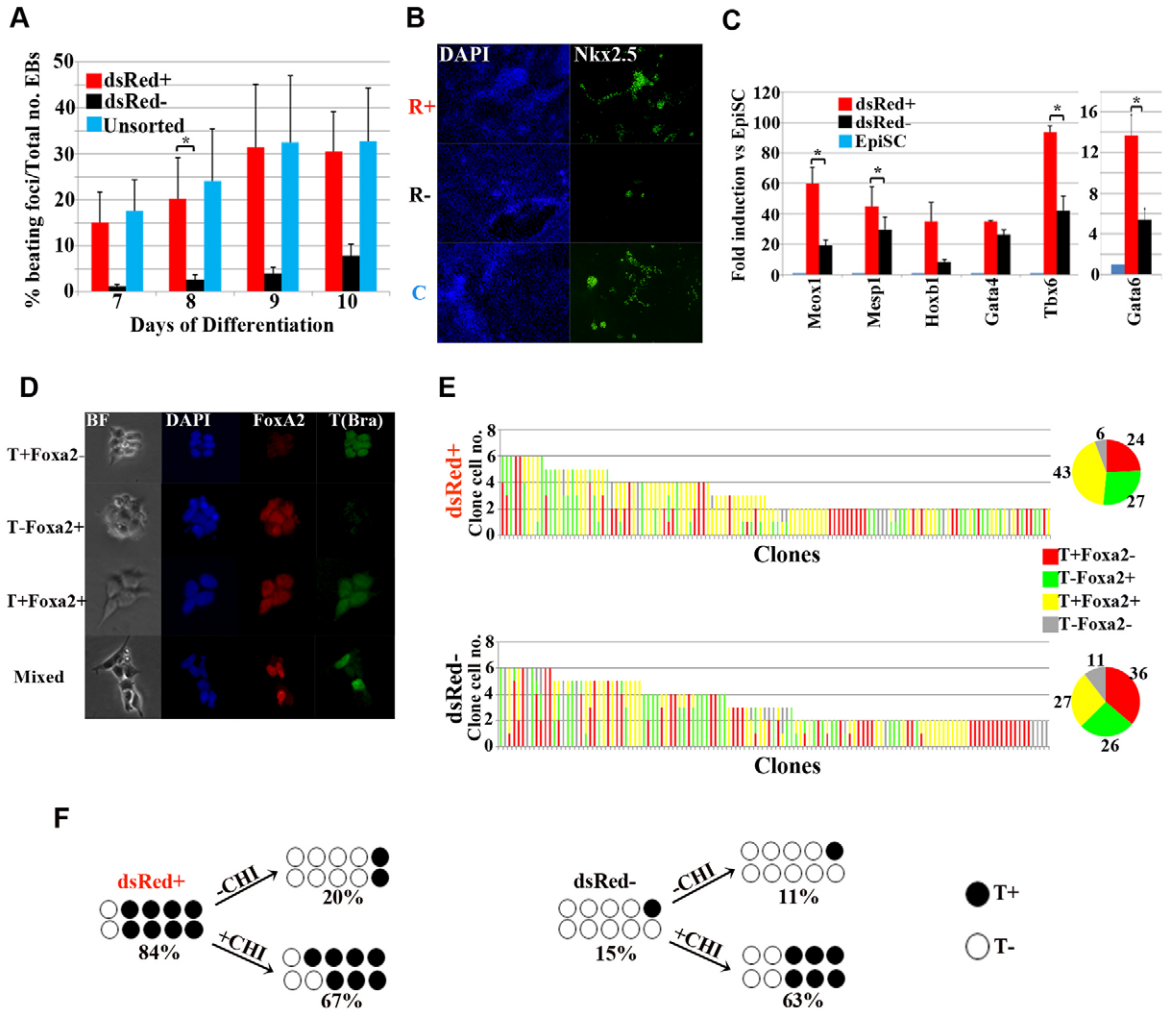

Fig. 4. Tps/tb promoter activity in EpiSCs correlates with distinct differentiation choices *in vitro*. (A) Cardiomyocyte differentiation expressed as percentage of beating foci/total plated EBs at different time points after sorting dsRed2$^+$ and dsRed2$^-$ EpiSCs. Unsorted EBs are included as a control. Error bars represent s.e.m. (n=3). *P<0.05 (Student's t-test). (B) Immunocytochemistry of Nkx2-5 expression in plated EBs derived from sorted dsRed2$^+$ and dsRed2$^-$ EpiSC fractions. (C) qPCR analysis of paraxial mesoderm and cardiac/endoderm marker expression in sorted dsRed2$^+$ and dsRed2$^-$ EpiSC-derived EBs. Values are expressed relative to undifferentiated EpiSCs. Error bars: s.e.m. (n=3). *P<0.05 (Student's t-test). (D) T(Bra) and Foxa2 immunofluorescence in colonies obtained after plating sorted Tps/tb-RED EpiSCs at clonal density for 48 hours in the presence of CHI. (E) Composition of colonies obtained after plating sorted dsRed2$^+$ and dsRed2$^-$ EpiSC at clonal density for 48 hours in CHI, depicted as in Fig. 2F. Number of clones: $N_{dsRed+clones}$=126, $N_{dsRed-clones}$=130. Pie charts: overall percentages of cells of each phenotype (number of cells: $N_{dsRed+cells}$=409, $N_{dsRed-cells}$=385). (F) Proportions of T(Bra)+ cells in steady-state dsRed2$^+$ and dsRed2$^-$ EpiSC populations (data from Fig. 1D) and after sorting and plating in EpiSC (data from Fig. 2F) or CHI treatment conditions (data from Fig. 4E). C, control.

markers was significantly enriched in dsRed2$^+$-derived EBs versus those from dsRed2$^-$ cells (Fig. 4C). By contrast, we did not observe any significant differences in the induction of endoderm-specific transcripts such as *Gsc*, *Sox17* and *Hex* (*Hhex* – Mouse Genome Informatics) within the same day 3 EBs between the two populations (supplementary material Fig. S8A). Moreover, in neural inducing conditions (Greber et al., 2010), sorted dsRed2$^+$ and dsRed2$^-$ cells did not exhibit significant differences in their ability to upregulate the neural markers *Sox1* and *Sox2* (supplementary material Fig. S8B). Thus dsRed2$^+$ cells show a strong bias towards mesodermal differentiation. However, consistent with the hypothesis that these cells are pluripotent EpiSCs, dsRed2$^+$ cells are still capable of generating endodermal and neural derivatives.

We next sought to define the potency of single dsRed2$^+$ and dsRed2$^-$ cells during CHI-mediated differentiation. Flow-sorted dsRed2$^+$ and negative EpiSCs were plated at clonal density in the presence of CHI, Activin A and Fgf2 and the induction of mesoderm and endoderm was assessed by scoring T(Bra)$^+$ and Foxa2$^+$ cells in the resulting colonies (Fig. 4D). After 48 hours' culture the majority of cells derived from both populations expressed T(Bra) protein to a similar extent (67% in dsRed2$^+$-derived cells versus 63% in dsRed2$^-$-derived cells) (Fig. 4E). Taken together with clonal data obtained in EpiSC conditions (Fig. 2F) and measurement of the starting proportions of T(Bra)$^+$ cells (Fig. 1D), these data indicate that cells plated at clonal density respond in a similar manner to the whole population (Fig. 2C, Fig. 3A) by re-equilibrating the proportions of T(Bra)$^+$ cells in EpiSC conditions, and dramatically increasing T(Bra)$^+$ cell numbers in +CHI conditions (Fig. 4F). In theory, these responses could have occurred by *de novo* induction of T(Bra), or by selection of pre-existing populations. The high frequency of heterogeneous clones (25% of both dsRed2$^+$ and dsRed2$^-$ clones), showing that individual cells could switch phenotypes, together with the similar numbers of clones, indicating that no condition selected against the majority of cells, and the even

Development (2014) doi:10.1242/dev.101014

distribution of T(Bra)$^+$ and T(Bra)$^-$ clone sizes, arguing against differential growth rates, all support the hypothesis that these populations are predominantly induced rather than arising by selection. However, live tracking of individual cells would be required to unequivocally distinguish these two possibilities.

dsRed2$^+$ cells generated significantly more double T(Bra)$^+$Foxa2$^+$ cells (43% from dsRed2$^+$ versus 27% from dsRed2$^-$, χ^2, P<0.01), whereas dsRed2$^-$ cells tended to generate T(Bra)$^+$ single positive cells (36% from dsRed2$^-$ versus 24% from dsRed2$^+$, χ^2, P<0.01; Fig. 4E). Most clones were homogeneous for these markers, but some (notably clones consisting of four or more cells) contained both T(Bra) and Foxa2 single positive cells (Fig. 4E), showing that a single cell can generate both T(Bra)$^+$ putative mesoderm and Foxa2$^+$ putative endoderm, especially after two or more divisions. Together, these findings suggest that upon Wnt activation, PS-like EpiSCs favour the production of mesendoderm-like T(Bra)$^+$Foxa2$^+$ cells, whereas the dsRed2$^-$ population preferentially generates T(Bra)$^+$ putative mesoderm.

Differentiation bias of PS-like EpiSCs *in vivo*

We have recently shown that mouse EpiSCs can be grafted into cultured gastrula stage embryos where they adopt cell identities instructed by their host environment in accordance with published fate maps (Huang et al., 2012). Thus, embryo grafting provides a stringent assay for testing how distinct cell populations respond to region-specific differentiation-inducing signals. To assess whether the *in vitro* lineage bias of PS-like EpiSCs is also evident *in vivo*, Tps/tb-RED EpiSCs constitutively expressing GFP (a line termed C2) (Huang et al., 2012) were FACS-sorted into dsRed2$^+$GFP$^+$ and dsRed2$^-$GFP$^+$ populations and grafted into two distinct sites of mid-to-late streak stage embryos, the anterior/distal part of the PS (ANT), which produces derivatives of all three germ layers, and the mid PS (MP), which principally gives rise to mesoderm and endoderm (Fig. 5A) (reviewed by Tam and Behringer, 1997). The recipient embryos were cultured for 24-48 hours and the incorporation of the two sorted fractions was assessed by fluorescence microscopy after sectioning (Fig. 5A). Most embryos developed normally (51/54, 94%) and contained GFP$^+$ cells after culture (50/51, 98%; Fig. 5C).

To compare the distribution of the grafted cell populations, we sectioned a subset (25/51) of the cultured embryos and scored GFP$^+$ cells in embryonic tissues, confirming correct differentiation using antibodies to T(Bra), Sox2 and Foxa2 (Fig. 5D). As reported previously for unsorted EpiSCs (Huang et al., 2012), both sorted fractions exhibited patterns of integration and differentiation consistent with published fate maps following engraftment (Fig. 5B; supplementary material Table S2). However, we also observed striking differences. dsRed2$^+$ cells showed a statistically significant, enhanced endodermal and axial mesodermal contribution (Fig. 5B) in either MP or both graft types, consistent with the close lineal relationship between axial mesoderm and endoderm progenitors *in vivo* (Kinder et al., 2001) (Fig. 5B). Conversely, dsRed2$^-$ cells colonised the PS and formed non-integrated clumps more frequently than dsRed2$^+$ cells following grafting into either region (Fig. 5B), suggesting that the integration of dsRed2$^-$ cells in the PS is impaired, leading to a delayed exit from this site (Fig. 5B). Despite their difference in endoderm and axial mesoderm contribution, both fractions appeared to incorporate to paraxial and lateral mesodermal tissues at a similar frequency (Fig. 5B). dsRed2$^-$ EpiSCs also showed marginally higher colonisation of the neural plate (NP) in either MP or ANT locations. Together these data indicate that the PS-like, dsRed2$^+$ EpiSC fraction is significantly biased towards PS derivatives *in vivo* (Fig. 5B). However, similar to the *in vitro* data, dsRed2$^+$ cells have not lost the ability to contribute to neurectoderm, consistent with a pluripotent status.

Wnt signalling stimulation in EpiSCs promotes ME and NM lineage restriction *in vivo*

We next examined whether the ME-like and NM-like populations induced by CHI treatment can produce functional cell types *in vivo*. C2 EpiSCs were treated with CHI for 48 hours and then grafted into the ANT region of mid-late streak embryos (Fig. 5A). Cultured host embryos were then analysed as above. Interestingly, we observed exclusive contribution of the donor cells to mesoderm and endoderm and complete absence of grafted cells from the neural plate (Fig. 5E). This finding implies that, in line with our *in vitro* data, elevated Wnt signalling abolishes EpiSC pluripotency, restricting differentiation, in the context of the gastrulation stage embryo, to mesoderm and endoderm fates. Moreover, paraxial and lateral mesoderm contribution was highly enriched in CHI-treated EpiSCs and axial mesoderm was not colonised at all (Fig. 5E), suggesting that high Wnt activity restricts the developmental potential of mesoderm progenitors.

The upregulation of somitogenesis stage markers in CHI-treated cultures (e.g. Hox paralogous groups 5-9; supplementary material Fig. S5E) prompted us to examine whether Wnt-stimulated EpiSC cultures include late PS progenitors. We have shown that EpiSCs fail to integrate into the NM progenitor-containing NSB of embryos that have initiated somitogenesis (Huang et al., 2012). Strikingly, CHI-treated C2 EpiSC integrated extensively into older embryos following engraftment into the E8.5 NSB in contrast to untreated EpiSCs (Fig. 5F). They colonised all embryos (6/6) analysed following culture while only one of four embryos grafted with untreated EpiSC exhibited minimal chimerism (Fig. 5F; data not shown). Importantly, the grafted CHI-treated cells differentiated predominantly into Pax3-positive somitic/paraxial mesoderm (Goulding et al., 1994), Snai2-positive lateral/ventral mesoderm (Sefton et al., 1998) and Pecam1-positive endothelia (Baldwin et al., 1994) (Fig. 5G). Moreover, in two recipient embryos, we detected GFP$^+$ cells in both the neural tube and somites, suggesting that CHI treatment can induce cells with neuromesodermal potency (Fig. 5G). Collectively, these findings show that Wnt signalling elevation drives differentiation of cells into mesoderm and endoderm lineages compatible with gastrulation stage embryos, and mesoderm and neural lineages compatible with somitogenesis stage embryos. This raises the possibility that the T(Bra)$^+$Foxa2$^+$ and T(Bra)$^+$Sox2$^+$ cells induced by CHI treatment are ME and NM progenitors, respectively.

DISCUSSION

Acquisition of lineage identity within primed pluripotency

Heterogeneity is prevalent in mouse and human pluripotent cell populations (Chambers et al., 2007; Canham et al., 2010; Blauwkamp et al., 2012; Davies et al., 2013) but few studies have focused on EpiSCs, and these have defined only minor (0.5-1.5%) functionally distinct subpopulations (Hayashi and Surani, 2009; Han et al., 2010). Here, we reveal the existence of two major EpiSC subpopulations, each representing up to 30% of the total EpiSC population, relevant to the gastrulating embryo: PS- and neural-like cells (Fig. 6). This plasticity in undifferentiated EpiSCs is reminiscent of the situation in the gastrula stage embryo, where the principal postimplantation pluripotency determinant Oct4 (Osorno et al., 2012) is expressed within cells that upregulate markers

Development (2014) doi:10.1242/dev.101014

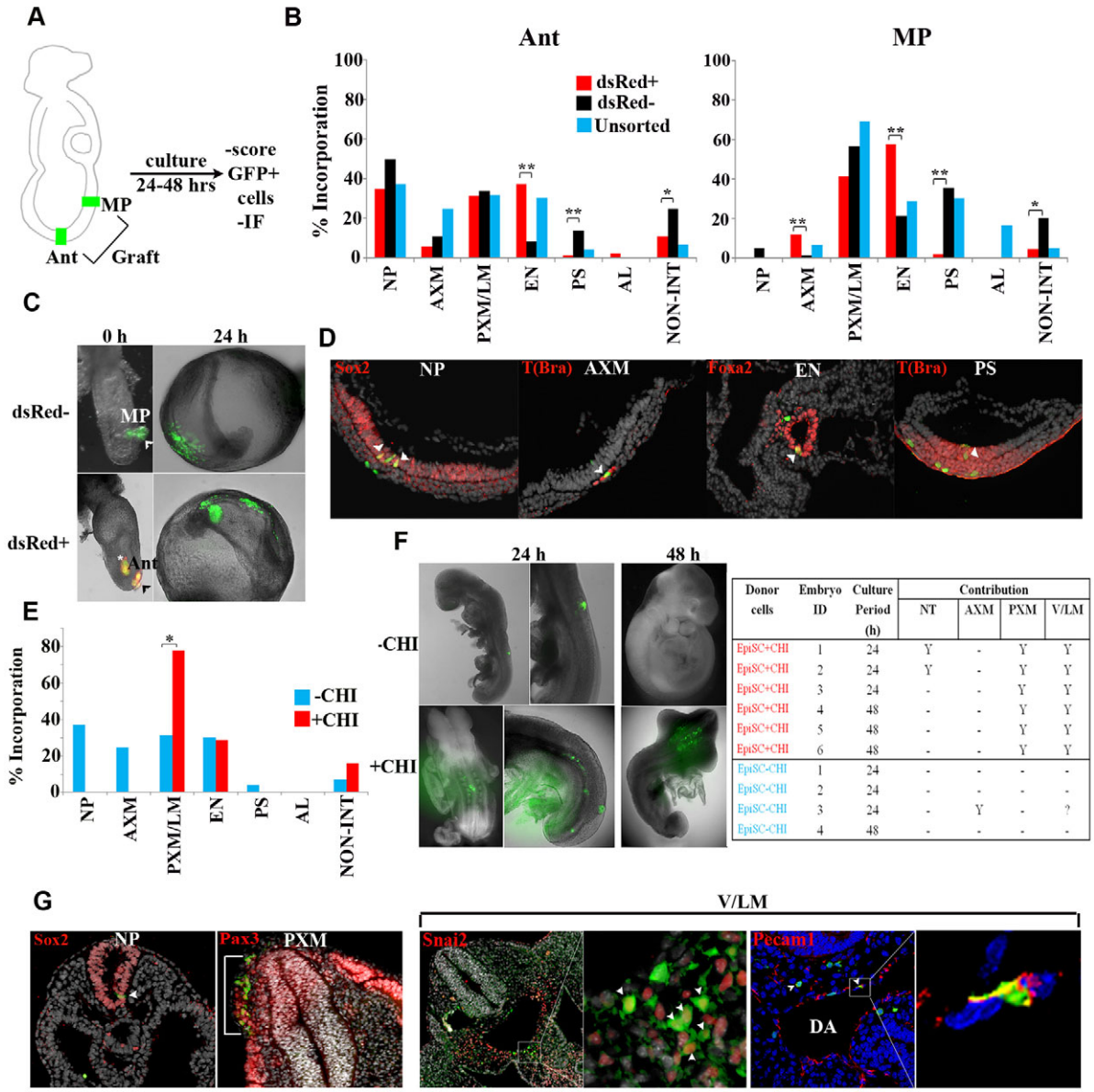

Donor cells	Embryo ID	Culture Period (h)	Contribution NT	AXM	PXM	V/LM
EpiSC+CHI	1	24	Y	-	Y	Y
EpiSC+CHI	2	24	Y	-	Y	Y
EpiSC+CHI	3	24	-	-	Y	Y
EpiSC+CHI	4	48	-	-	Y	Y
EpiSC+CHI	5	48	-	-	Y	Y
EpiSC+CHI	6	48	-	-	Y	Y
EpiSC-CHI	1	24	-	-	-	-
EpiSC-CHI	2	24	-	-	-	-
EpiSC-CHI	3	24	-	Y	-	?
EpiSC-CHI	4	48	-	-	-	-

Fig. 5. Tps/tb promoter activity in EpiSCs correlates with distinct differentiation choices *in vivo*. (A) Diagram showing graft sites in mid-late streak embryo (mid-posterior, MP; and anterior streak, Ant). (B) Extent of incorporation (percentage of sections containing donor cells/total sections) after grafting sorted dsRed2^{+}GFP^{+}, dsRed2^{-}GFP^{+} or unsorted GFP^{+} EpiSCs into the indicated sites. *P*-values were calculated using the χ^2 test. For Ant grafts: N_{dsRed+}=4, N_{dsRed-}=5, $N_{unsorted}$=2). For MP grafts: N_{dsRed+}=4, N_{dsRed-}=4, $N_{unsorted}$=4). **P*<0.05; ***P*<0.01 (chi-squared test). See supplementary material Table S2 for individual embryo data. (C) Representative examples of M-LS embryo grafts (0 hours) and distribution of sorted dsRed2^{+}GFP^{+} and dsRed2^{-}GFP^{+} EpiSCs after 24 hours embryo culture. Arrowheads, graft sites. Asterisk, clump in amniotic cavity. (D) Representative examples of donor cell incorporation (green, GFP) and differentiation (red, immunofluorescence for indicated markers). Grey, 4′,6-diamidino-2-phenylindole (DAPI) counterstain. Arrowheads, co-expressing donor cells. Note: dsRed2 expression was undetectable after 48-hour culture in the absence of doxycycline. (E) Extent of incorporation after grafting of CHI-treated GFP^{+} EpiSCs into the anterior PS of M-LS stage embryos. Note: untreated control frequencies reproduced from B (**P*<0.01; N_{+CHI}=4, $N_{unsorted}$=2). (F,G) Grafting of C2 EpiSCs ±CHI treatment to E8.5 embryos and culture for 24-48 hours. (F) Left, representative embryos and right, donor cell contribution. (G) Green, GFP immunofluorescence; red, indicated marker immunofluorescence in representative sections after culture; blue or grey, DAPI counterstain. Note that the images depicting NP and PXM contribution belong to the same embryo. Arrowheads, co-expressing donor cell. AL, allantois; Ant, anterior streak; AXM, axial mesoderm; DA, dorsal aorta; EN, endoderm; MP, mid posterior; NON-INT, non-integrated cell clumps; NP, neural plate; PXM/LM, paraxial/lateral mesoderm; PS, primitive streak; V/LM, ventral/lateral mesoderm.

characteristic of the lineage(s) they are fated to generate (Teo et al., 2011; Cajal et al., 2012; Osorno et al., 2012). Teratocarcinoma formation and heterotopic grafting experiments indicate that although cell fate during gastrulation is regionalised, epiblast cells remain pluripotent until the beginning of somitogenesis (Beddington, 1981; Beddington, 1982; Beddington, 1983; Osorno et al., 2012). Our observation of lineage-biased EpiSC subpopulations suggests that regionalised epiblast populations have begun the process of lineage specification, but that these PS-like or neural-like states are initially reversible. In EpiSCs, these events do not lead to lineage commitment, probably because of the constraints imposed upon the cells by the pluripotency-promoting culture conditions, raising the possibility that similar constraints may act upon the gastrulation stage epiblast.

Development (2014) doi:10.1242/dev.101014

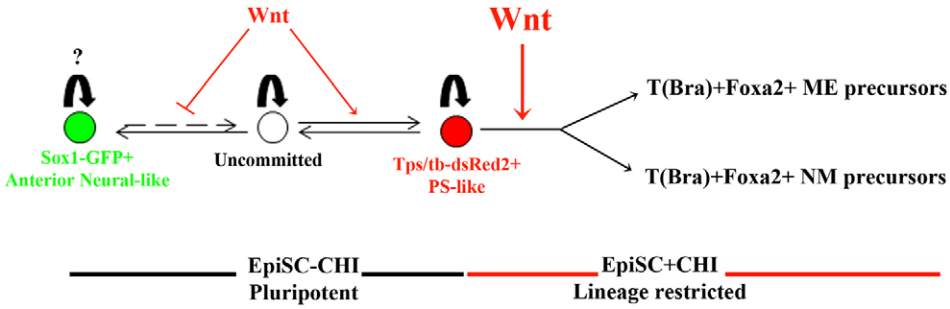

Fig. 6. Model of PS precursor specification *in vitro*. Undifferentiated EpiSC cultures contain two major mutually exclusive subpopulations: a Wnt/β-catenin-low partially committed neural-like and a PS-biased pluripotent, reversible fraction marked by slightly higher Wnt levels. Further elevation of Wnt/β-catenin signalling above this pluripotency-compatible Wnt activity threshold promotes the generation of lineage-restricted populations resembling mesendodermal (ME) and neuromesodermal (NM) precursors. Red arrows, Wnt effects.

Wnt signalling as a driver of plastic PS-like identity in undifferentiated EpiSC

In vivo, Wnt/β-catenin signalling has been implicated in the initiation of PS formation (Liu et al., 1999; Kelly et al., 2004; Mohamed et al., 2004) and the establishment, in collaboration with T(Bra), of a 'mesodermal progenitor niche' in zebrafish (Martin and Kimelman, 2010). Our data showing that Wnt/β-catenin signalling promotes a PS-like population *in vitro* are in line with these findings as well as a number of other studies demonstrating that Wnt/β-catenin drives PS-like differentiation *in vitro* (Faunes et al., 2013; Blauwkamp et al., 2012; Sumi et al., 2013; Kim et al., 2013). However, our study distinguishes two separate roles of Wnt/β-catenin signalling. Low Wnt activity in self-renewing EpiSCs is sufficient to impose a reversible, pluripotent, early PS character; elevation of Wnt signalling levels above this pluripotency-permissive threshold via CHI treatment drives commitment to mesodermal/endodermal and posterior neural/mesodermal fates (Fig. 6). We also provide evidence that Wnt/β-catenin signalling represses anterior epiblast/early neural features (Fig. 6, Fig. 3F). A recent study examining multiple EpiSC lines has revealed that a Wnt signalling gene expression signature characterises the EpiSC transcriptome, potentially contributing to the acquisition of a PS character (Kojima et al., 2014). Interestingly, self-renewing EpiSCs are also marked by the activity of a pro-anterior neural plate transcriptional network that includes Otx2 and Sox2, stabilising an undifferentiated EpiSC state by repressing mesodermal/endodermal differentiation (Iwafuchi-Doi et al., 2012). Our data integrate these findings, showing that early anterior neural and PS-like subpopulations coexist within self-renewing EpiSC cultures and that Wnt/β-catenin activity limits the former while stimulating the latter (Fig. 6, Fig. 3F).

High levels of Wnt signalling generate two distinct PS-derived precursor populations

T(Bra)$^+$Foxa2$^+$ ME precursors that can generate cardiac mesoderm and endoderm have been previously described in Wnt-induced ESC differentiation (Kubo et al., 2004; Gadue et al., 2006). Our data show that similar cells are frequent in PS-like dsRed2$^+$ EpiSCs (Fig. 1D). The preferential contribution of sorted dsRed2$^+$ EpiSCs to endoderm *in vivo* (Fig. 5B) and the increased frequency of T(Bra)$^+$Foxa2$^+$ cells from single dsRed2$^+$ cells in the presence of CHI (Fig. 4E) also suggest that the acquisition of PS characteristics by undifferentiated EpiSCs is the earliest 'entry point' of commitment to an ME precursor state. Thus in the embryonic PS, ME-like dsRed2$^+$ cells may integrate and exit from this region more efficiently than dsRed2$^-$ cells, and as a consequence favour endoderm, an early PS derivative. Conversely, CHI treatment of dsRed2$^-$ cells, which favours production of T(Bra)$^+$ putative mesoderm over T(Bra)$^+$Foxa2$^+$ ME cells, offers an explanation for the discrepancy between *in vitro* data showing that in EB differentiation dsRed2$^-$ cells are biased against mesoderm differentiation, whereas they efficiently produce mesoderm *in vivo*. The PS, a natural source of Wnt signals, may induce mesoderm in preference to endoderm in dsRed2$^-$ cells. Furthermore, the increased paraxial mesoderm differentiation *in vivo* exhibited by CHI-treated cells (Fig. 5E) probably results from its induction of T(Bra)$^+$ mesoderm precursors from dsRed2$^-$ cells, as these constitute the majority of steady-state Tps/tb-RED EpiSC cultures.

Co-expression of T(Bra) and Sox2 marks NM progenitors in various vertebrates (Martin and Kimelman, 2012; Olivera-Martinez et al., 2012) and our data confirm this in the mouse (supplementary material Fig. S7). We also demonstrate that elevated Wnt signalling leads to the generation of T(Bra)$^+$Sox2$^+$ cells *in vitro* that are distinct from T(Bra)$^+$Foxa2$^+$ putative ME progenitors. The specific upregulation of posterior but not anterior neurectodermal markers, the induction of trunk Hox genes and the neuromesodermal contribution of CHI-treated EpiSCs after engraftment into the NSB of some embryos support the hypothesis that Wnt-driven T/Sox2 co-expression also marks NM-potent cells *in vitro*. The generation of the two mutually exclusive (Bra)$^+$Foxa2$^+$ (ME-like) and T(Bra)$^+$Sox2$^+$ (NM-like) entities upon EpiSC differentiation is in agreement with retrospective clonal analysis data from the mouse embryo showing that early-ingressing mesodermal types such as cardiac mesoderm can arise from a common ME precursor while the later-ingressing paraxial mesoderm is produced by a common NM progenitor (Tzouanacou et al., 2009). Our data underline the similarity between EpiSCs and the gastrulation stage epiblast, implying that EpiSCs can be used as a physiologically relevant system to study events during gastrulation *in vitro*.

MATERIALS AND METHODS

Cell culture and differentiation

Feeder-free EpiSCs were derived from ESCs (Guo et al., 2009) or embryonic day (E) 6.5 embryos (Osorno et al., 2012) and maintained as described previously (Osorno et al., 2012). Tps/tb-RED EpiSCs were generated from an ESC line containing a randomly integrated PS- and tail bud-specific 1.2 kb *T*(*Bra*) promoter fragment (Clements et al., 1996) driving the reverse tetracycline transactivator rtTA2^S-M2 and a tet-responsive element-linked dsRed2 transgene knocked into the *hprt* locus. The parental ESC line (C.E., A.T. and V.W., unpublished) will be described in detail elsewhere. dsRed2 expression was induced and maintained by continuous culture in doxycycline (1 µg/ml; Sigma). *Ctnnb1* null EpiSCs were established after 4-hydroxytamoxifen treatment following

differentiation from ESCs derived from a mouse line containing two floxed *Ctnnb1* alleles, a floxed phosphoglycerate kinase-GFP (Pgk-GFP) cassette and the Cre-ER^{T2} transgene knocked into the ROSA26 locus (supplementary material Fig. S6) (Brault et al., 2001; Gilchrist et al., 2003). For cardiomyocyte differentiation ~10^6 cells were cultured in suspension in Glasgow minimum essential medium (GMEM) + 10% fetal calf serum for 4 days followed by transfer of EBs to gelatinised wells of 24-well plates (5-10 EBs/well). For inhibition and neural differentiation experiments, cells were plated in the presence of the MEK-Erk inhibitor PD0325901 (1 μM; Signal Transduction Division, Dundee, UK) and the Tgfβ/Nodal inhibitor SB431542 (10 μM; Sigma) (~350,000/well in 6-well plates) for 48-72 hours. To inhibit Wnt signalling, EpiSC cultures were treated for 5 days with recombinant human Wif1 (0.8 μg/ml, R&D Systems) with daily media changes. To stimulate Wnt signalling, cells cultured on fibronectin-coated wells (Sigma) were treated for 48-72 hours with CHIRON99021 (3 μM, Signal Transduction Division, Dundee) or Wnt3a (50 ng/ml, R&D Systems). For clonal density experiments, cells were plated at 10,000 cells/well in 6-well plates. Using a 1:1 mixture of GFP$^+$ and GFP$^-$ cells we confirmed that, at this density, 95% of the resulting colonies consisting of two to eight cells are of monoclonal origin.

Embryo grafting and scoring

Embryo grafting, culture and imaging was performed as described (Huang et al., 2012) using either 48-hour CHI-treated or flow-sorted EpiSCs, the latter plated overnight in four-well dishes in standard EpiSC conditions, to allow coherent cell clumps to form.

RNA analysis and microarrays

RNA isolation, cDNA synthesis and real-time qPCR expression analysis were performed as described previously (Osorno et al., 2012). Each biological replicate in qPCR experiments comprised three technical replicates. For microarrays, total RNA from three biological replicates was isolated and labelled/amplified using the Illumina TotalPrep RNA Amplification Kit (Life Technologies). Whole genome expression profiling was performed using Illumina MouseWG-6 v2 arrays (Edinburgh Wellcome Trust Clinical Research Facility). Microarray analysis was performed in the R statistical environment using the lumi package (Du et al., 2008). Data pre-processing was performed using background subtraction, variance stabilising transformation (VST) and robust spline normalisation (RSN). Differentially expressed genes were identified using the limma package with fold-change (FC) ≥1.5 and FDR ≤0.05 (Smyth, 2005). The raw data have been deposited in GEO with accession number GSE48476.

Immunocytochemistry

Immunocytochemistry was performed as described previously (Osorno et al., 2012). Primary antibody concentrations were: anti-Nanog, 2.5 μg/ml (14-5761-80, eBioscience); anti-Oct4, 1 μg/ml (N-19, Santa Cruz); anti-Sox2, 0.5 μg/ml (Y-17, Santa Cruz) or 1:200 (ab92494, Abcam); anti-Foxa2, 2 μg/ml (M-20, Santa Cruz) or 1:200 (ab40874, Abcam); anti-Gsc 2 μg/ml (N-12, Santa Cruz); anti-T (Bra), 1 μg/ml (AF2085, R&D); anti-Cdh1, 0.4 μg/ml (ECCD2, Calbiochem); anti-Cdh2, 5 μg/ml (8C11, BD Biosciences); anti-Nes, 1:20 (Rat-401, DSHB); anti-Nkx2.5, 20 μg/ml (ab35842, Abcam); anti-CD31, 4 μg/ml (MEC 13.3, BD Pharmingen).

Imaging and image analysis

Fluorescence in cultured cells was visualised using an Olympus IX51 inverted microscope (Olympus) or an inverted Confocal Leica TCS SPE microscope after culture on fibronectin-coated glass coverslips. Whole embryos were imaged using a Nikon NZ100 dissecting microscope, and sections were imaged in an Olympus BX61 fluorescence compound microscope. Images were captured using Volocity software (PerkinElmer). Nuclear segmentation followed by single cell fluorescence quantification was performed as described previously (Osorno et al., 2012).

Flow cytometry

Flow cytometry analysis was performed using a FACSCalibur (BD Biosciences) cytometer. Cell sorting was performed using a FACSAria (BD Biosciences). For interconversion and clonal plating experiments, cells were treated for 30 minutes with the ROCK inhibitor Y-27632 (10 μM; Calbiochem) before dispersal and for 24 hours after sorting.

Acknowledgements

We thank Simon Monard, Olivia Rodrigues, Fiona Rossi, Shonna Johnston, Lynsey Robertson and Valeria Berno for technical assistance; Luke Boulter, Celine Souilhol, Alexander Medvinsky, Andrew Smith, Simon Tomlinson, Andreas Tsakiridis and Anne Wiblin for advice and reagents; and Keisuke Kaji, Hisato Kondoh and Ian Chambers for critical reading of the manuscript.

Competing interests

The authors declare no competing financial interests.

Author contributions

A.T. designed and carried out experiments and prepared the manuscript with V.W.; Y.H. performed embryo grafting experiments; G.B. analysed the 46C EpiSC line; F.W. and E.K. provided immunostaining data; S.Z. generated the fl/fl Ctnnb1 mouse line; R.O. generated the fl/fl-Ctnnb1 and Δ/Δ-Ctnnb1 EpiSC lines; C.E. generated the Tps/tb-RED ESC line; S.S. performed microarray analysis; S.L. supervised experiments.

Funding

This work was supported by the Association for International Cancer Research [08-0493]; and the Medical Research Council [G080297 and MR/K011200]. Deposited in PMC for immediate release.

Supplementary material

Supplementary material available online at
http://dev.biologists.org/lookup/suppl/doi:10.1242/dev.101014/-/DC1

References

Acampora, D., Di Giovannantonio, L. G. and Simeone, A. (2013). Otx2 is an intrinsic determinant of the embryonic stem cell state and is required for transition to a stable epiblast stem cell condition. *Development* **140**, 43-55.

Arnold, S. J. and Robertson, E. J. (2009). Making a commitment: cell lineage allocation and axis patterning in the early mouse embryo. *Nat. Rev. Mol. Cell Biol.* **10**, 91-103.

Arnold, S. J., Stappert, J., Bauer, A., Kispert, A., Herrmann, B. G. and Kemler, R. (2000). Brachyury is a target gene of the Wnt/beta-catenin signaling pathway. *Mech. Dev.* **91**, 249-258.

Baldwin, H. S., Shen, H. M., Yan, H. C., DeLisser, H. M., Chung, A., Mickanin, C., Trask, T., Kirschbaum, N. E., Newman, P. J., Albelda, S. M. et al. (1994). Platelet endothelial cell adhesion molecule-1 (PECAM-1/CD31): alternatively spliced, functionally distinct isoforms expressed during mammalian cardiovascular development. *Development* **120**, 2539-2553.

Beddington, S. P. (1981). An autoradiographic analysis of the potency of embryonic ectoderm in the 8th day postimplantation mouse embryo. *J. Embryol. Exp. Morphol.* **64**, 87-104.

Beddington, R. S. (1982). An autoradiographic analysis of tissue potency in different regions of the embryonic ectoderm during gastrulation in the mouse. *J. Embryol. Exp. Morphol.* **69**, 265-285.

Beddington, R. S. (1983). Histogenetic and neoplastic potential of different regions of the mouse embryonic egg cylinder. *J. Embryol. Exp. Morphol.* **75**, 189-204.

Ben-Haim, N., Lu, C., Guzman-Ayala, M., Pescatore, L., Mesnard, D., Bischofberger, M., Naef, F., Robertson, E. J. and Constam, D. B. (2006). The nodal precursor acting via activin receptors induces mesoderm by maintaining a source of its convertases and BMP4. *Dev. Cell* **11**, 313-323.

Bernemann, C., Greber, B., Ko, K., Sterneckert, J., Han, D. W., Araúzo-Bravo, M. J. and Schöler, H. R. (2011). Distinct developmental ground states of epiblast stem cell lines determine different pluripotency features. *Stem Cells* **29**, 1496-1503.

Blauwkamp, T. A., Nigam, S., Ardehali, R., Weissman, I. L. and Nusse, R. (2012). Endogenous Wnt signalling in human embryonic stem cells generates an equilibrium of distinct lineage-specified progenitors. *Nat. Commun.* **3**, 1070.

Brault, V., Moore, R., Kutsch, S., Ishibashi, M., Rowitch, D. H., McMahon, A. P., Sommer, L., Boussadia, O. and Kemler, R. (2001). Inactivation of the beta-catenin gene by Wnt1-Cre-mediated deletion results in dramatic brain malformation and failure of craniofacial development. *Development* **128**, 1253-1264.

Brons, I. G., Smithers, L. E., Trotter, M. W., Rugg-Gunn, P., Sun, B., Chuva de Sousa Lopes, S. M., Howlett, S. K., Clarkson, A., Ahrlund-Richter, L., Pedersen, R. A. et al. (2007). Derivation of pluripotent epiblast stem cells from mammalian embryos. *Nature* **448**, 191-195.

Burtscher, I. and Lickert, H. (2009). Foxa2 regulates polarity and epithelialization in the endoderm germ layer of the mouse embryo. *Development* **136**, 1029-1038.

Cajal, M., Lawson, K. A., Hill, B., Moreau, A., Rao, J., Ross, A., Collignon, J. and Camus, A. (2012). Clonal and molecular analysis of the prospective anterior neural boundary in the mouse embryo. *Development* **139**, 423-436.

Cambray, N. and Wilson, V. (2007). Two distinct sources for a population of maturing axial progenitors. *Development* **134**, 2829-2840.

Candia, A. F., Hu, J., Crosby, J., Lalley, P. A., Noden, D., Nadeau, J. H. and Wright, C. V. (1992). Mox-1 and Mox-2 define a novel homeobox gene subfamily and are differentially expressed during early mesodermal patterning in mouse embryos. *Development* **116**, 1123-1136.
Canham, M. A., Sharov, A. A., Ko, M. S. and Brickman, J. M. (2010). Functional heterogeneity of embryonic stem cells revealed through translational amplification of an early endodermal transcript. *PLoS Biol.* **8**, e1000379.
Chambers, I., Silva, J., Colby, D., Nichols, J., Nijmeijer, B., Robertson, M., Vrana, J., Jones, K., Grotewold, L. and Smith, A. (2007). Nanog safeguards pluripotency and mediates germline development. *Nature* **450**, 1230-1234.
Chapman, D. L., Agulnik, I., Hancock, S., Silver, L. M. and Papaioannou, V. E. (1996). Tbx6, a mouse T-Box gene implicated in paraxial mesoderm formation at gastrulation. *Dev. Biol.* **180**, 534-542.
Clements, D., Taylor, H. C., Herrmann, B. G. and Stott, D. (1996). Distinct regulatory control of the Brachyury gene in axial and non-axial mesoderm suggests separation of mesoderm lineages early in mouse gastrulation. *Mech. Dev.* **56**, 139-149.
Conlon, F. L., Lyons, K. M., Takaesu, N., Barth, K. S., Kispert, A., Herrmann, B. and Robertson, E. J. (1994). A primary requirement for nodal in the formation and maintenance of the primitive streak in the mouse. *Development* **120**, 1919-1928.
Davies, O. R., Lin, C. Y., Radzisheuskaya, A., Zhou, X., Taube, J., Blin, G., Waterhouse, A., Smith, A. J. and Lowell, S. (2013). Tcf15 primes pluripotent cells for differentiation. *Cell Rep.* **3**, 472-484.
Deschamps, J., van den Akker, E., Forlani, S., De Graaff, W., Oosterveen, T., Roelen, B. and Roelfsema, J. (1999). Initiation, establishment and maintenance of Hox gene expression patterns in the mouse. *Int. J. Dev. Biol.* **43**, 635-650.
Du, P., Kibbe, W. A. and Lin, S. M. (2008). lumi: a pipeline for processing Illumina microarray. *Bioinformatics* **24**, 1547-1548.
Faunes, F., Hayward, P., Descalzo, S. M., Chatterjee, S. S., Balayo, T., Trott, J., Christoforou, A., Ferrer-Vaquer, A., Hadjantonakis, A. K., Dasgupta, R. et al. (2013). A membrane-associated β-catenin/Oct4 complex correlates with ground-state pluripotency in mouse embryonic stem cells. *Development* **140**, 1171-1183.
Forlani, S., Lawson, K. A. and Deschamps, J. (2003). Acquisition of Hox codes during gastrulation and axial elongation in the mouse embryo. *Development* **130**, 3807-3819.
Gadue, P., Huber, T. L., Paddison, P. J. and Keller, G. M. (2006). Wnt and TGF-beta signaling are required for the induction of an in vitro model of primitive streak formation using embryonic stem cells. *Proc. Natl. Acad. Sci. USA* **103**, 16806-16811.
Gamer, L. W. and Wright, C. V. (1993). Murine Cdx-4 bears striking similarities to the Drosophila caudal gene in its homeodomain sequence and early expression pattern. *Mech. Dev.* **43**, 71-81.
Gilchrist, D. S., Ure, J., Hook, L. and Medvinsky, A. (2003). Labeling of hematopoietic stem and progenitor cells in novel activatable EGFP reporter mice. *Genesis* **36**, 168-176.
Goulding, M., Lumsden, A. and Paquette, A. J. (1994). Regulation of Pax-3 expression in the dermomyotome and its role in muscle development. *Development* **120**, 957-971.
Greber, B., Wu, G., Bernemann, C., Joo, J. Y., Han, D. W., Ko, K., Tapia, N., Sabour, D., Sterneckert, J., Tesar, P. et al. (2010). Conserved and divergent roles of FGF signaling in mouse epiblast stem cells and human embryonic stem cells. *Cell Stem Cell* **6**, 215-226.
Grindley, J. C., Davidson, D. R. and Hill, R. E. (1995). The role of Pax-6 in eye and nasal development. *Development* **121**, 1433-1442.
Guo, G., Yang, J., Nichols, J., Hall, J. S., Eyres, I., Mansfield, W. and Smith, A. (2009). Klf4 reverts developmentally programmed restriction of ground state pluripotency. *Development* **136**, 1063-1069.
Han, D. W., Tapia, N., Joo, J. Y., Greber, B., Araúzo-Bravo, M. J., Bernemann, C., Ko, K., Wu, G., Stehling, M., Do, J. T. et al. (2010). Epiblast stem cell subpopulations represent mouse embryos of distinct pregastrulation stages. *Cell* **143**, 617-627.
Hayashi, K. and Surani, M. A. (2009). Self-renewing epiblast stem cells exhibit continual delineation of germ cells with epigenetic reprogramming in vitro. *Development* **136**, 3549-3556.
Hsieh, J. C., Kodjabachian, L., Rebbert, M. L., Rattner, A., Smallwood, P. M., Samos, C. H., Nusse, R., Dawid, I. B. and Nathans, J. (1999). A new secreted protein that binds to Wnt proteins and inhibits their activities. *Nature* **398**, 431-436.
Huang, Y., Osorno, R., Tsakiridis, A. and Wilson, V. (2012). In Vivo differentiation potential of epiblast stem cells revealed by chimeric embryo formation. *Cell Rep.* **2**, 1571-1578.
Inman, G. J., Nicolás, F. J., Callahan, J. F., Harling, J. D., Gaster, L. M., Reith, A. D., Laping, N. J. and Hill, C. S. (2002). SB-431542 is a potent and specific inhibitor of transforming growth factor-beta superfamily type I activin receptor-like kinase (ALK) receptors ALK4, ALK5, and ALK7. *Mol. Pharmacol.* **62**, 65-74.
Iwafuchi-Doi, M., Matsuda, K., Murakami, K., Niwa, H., Tesar, P. J., Aruga, J., Matsuo, I. and Kondoh, H. (2012). Transcriptional regulatory networks in epiblast cells and during anterior neural plate development as modeled in epiblast stem cells. *Development* **139**, 3926-3937.
Kelly, O. G., Pinson, K. I. and Skarnes, W. C. (2004). The Wnt co-receptors Lrp5 and Lrp6 are essential for gastrulation in mice. *Development* **131**, 2803-2815.
Kim, H., Wu, J., Ye, S., Tai, C. I., Zhou, X., Yan, H., Li, P., Pera, M. and Ying, Q. L. (2013). Modulation of β-catenin function maintains mouse epiblast stem cell and human embryonic stem cell self-renewal. *Nat. Commun.* **4**, 2403.
Kinder, S. J., Tsang, T. E., Quinlan, G. A., Hadjantonakis, A. K., Nagy, A. and Tam, P. P. (1999). The orderly allocation of mesodermal cells to the extraembryonic structures and the anteroposterior axis during gastrulation of the mouse embryo. *Development* **126**, 4691-4701.
Kinder, S. J., Tsang, T. E., Wakamiya, M., Sasaki, H., Behringer, R. R., Nagy, A. and Tam, P. P. (2001). The organizer of the mouse gastrula is composed of a dynamic population of progenitor cells for the axial mesoderm. *Development* **128**, 3623-3634.
Kispert, A. and Herrmann, B. G. (1994). Immunohistochemical analysis of the Brachyury protein in wild-type and mutant mouse embryos. *Dev. Biol.* **161**, 179-193.
Kojima, Y., Kaufman-Francis, K., Studdert, J. B., Steiner, K. A., Power, M. D., Loebel, D. A., Jones, V., Hor, A., de Alencastro, G., Logan, G. J. et al. (2014). The transcriptional and functional properties of mouse epiblast stem cells resemble the anterior primitive streak. *Cell Stem Cell* **14**, 107-120.
Kubo, A., Shinozaki, K., Shannon, J. M., Kouskoff, V., Kennedy, M., Woo, S., Fehling, H. J. and Keller, G. (2004). Development of definitive endoderm from embryonic stem cells in culture. *Development* **131**, 1651-1662.
Latinkić, B. V., Umbhauer, M., Neal, K. A., Lerchner, W., Smith, J. C. and Cunliffe, V. (1997). The Xenopus Brachyury promoter is activated by FGF and low concentrations of activin and suppressed by high concentrations of activin and by paired-type homeodomain proteins. *Genes Dev.* **11**, 3265-3276.
Lawson, K. A. (1999). Fate mapping the mouse embryo. *Int. J. Dev. Biol.* **43**, 773-775.
Lawson, K. A., Meneses, J. J. and Pedersen, R. A. (1991). Clonal analysis of epiblast fate during germ layer formation in the mouse embryo. *Development* **113**, 891-911.
Lee, K. L., Lim, S. K., Orlov, Y. L., Yit, Y., Yang, H., Ang, L. T., Poellinger, L. and Lim, B. (2011). Graded Nodal/Activin signaling titrates conversion of quantitative phospho-Smad2 levels into qualitative embryonic stem cell fate decisions. *PLoS Genet.* **7**, e1002130.
Lendahl, U., Zimmerman, L. B. and McKay, R. D. (1990). CNS stem cells express a new class of intermediate filament protein. *Cell* **60**, 585-595.
Liu, P., Wakamiya, M., Shea, M. J., Albrecht, U., Behringer, R. R. and Bradley, A. (1999). Requirement for Wnt3 in vertebrate axis formation. *Nat. Genet.* **22**, 361-365.
Lyashenko, N., Winter, M., Migliorini, D., Biechele, T., Moon, R. T. and Hartmann, C. (2011). Differential requirement for the dual functions of β-catenin in embryonic stem cell self-renewal and germ layer formation. *Nat. Cell Biol.* **13**, 753-761.
Martin, B. L. and Kimelman, D. (2010). Brachyury establishes the embryonic mesodermal progenitor niche. *Genes Dev.* **24**, 2778-2783.
Martin, B. L. and Kimelman, D. (2012). Canonical Wnt signaling dynamically controls multiple stem cell fate decisions during vertebrate body formation. *Dev. Cell* **22**, 223-232.
Mohamed, O. A., Clarke, H. J. and Dufort, D. (2004). Beta-catenin signaling marks the prospective site of primitive streak formation in the mouse embryo. *Dev. Dyn.* **231**, 416-424.
Morrisey, E. E., Ip, H. S., Lu, M. M. and Parmacek, M. S. (1996). GATA-6: a zinc finger transcription factor that is expressed in multiple cell lineages derived from lateral mesoderm. *Dev. Biol.* **177**, 309-322.
Murray, J. T., Campbell, D. G., Morrice, N., Auld, G. C., Shpiro, N., Marquez, R., Peggie, M., Bain, J., Bloomberg, G. B., Grahammer, F. et al. (2004). Exploitation of KESTREL to identify NDRG family members as physiological substrates for SGK1 and GSK3. *Biochem. J.* **384**, 477-488.
Olivera-Martinez, I., Harada, H., Halley, P. A. and Storey, K. G. (2012). Loss of FGF-dependent mesoderm identity and rise of endogenous retinoid signalling determine cessation of body axis elongation. *PLoS Biol.* **10**, e1001415.
Osorno, R., Tsakiridis, A., Wong, F., Cambray, N., Economou, C., Wilkie, R., Blin, G., Scotting, P. J., Chambers, I. and Wilson, V. (2012). The developmental dismantling of pluripotency is reversed by ectopic Oct4 expression. *Development* **139**, 2288-2298.
Pfister, S., Steiner, K. A. and Tam, P. P. (2007). Gene expression pattern and progression of embryogenesis in the immediate post-implantation period of mouse development. *Gene Expr. Patterns* **7**, 558-573.
Radice, G. L., Rayburn, H., Matsunami, H., Knudsen, K. A., Takeichi, M. and Hynes, R. O. (1997). Developmental defects in mouse embryos lacking N-cadherin. *Dev. Biol.* **181**, 64-78.
Ring, D. B., Johnson, K. W., Henriksen, E. J., Nuss, J. M., Goff, D., Kinnick, T. R., Ma, S. T., Reeder, J. W., Samuels, I., Slabiak, T. et al. (2003). Selective glycogen synthase kinase 3 inhibitors potentiate insulin activation of glucose transport and utilization in vitro and in vivo. *Diabetes* **52**, 588-595.
Rivera-Pérez, J. A. and Magnuson, T. (2005). Primitive streak formation in mice is preceded by localized activation of Brachyury and Wnt3. *Dev. Biol.* **288**, 363-371.
Saga, Y., Miyagawa-Tomita, S., Takagi, A., Kitajima, S., Miyazaki, J. and Inoue, T. (1999). MesP1 is expressed in the heart precursor cells and required for the formation of a single heart tube. *Development* **126**, 3437-3447.
Sasaki, H. and Hogan, B. L. (1993). Differential expression of multiple fork head related genes during gastrulation and axial pattern formation in the mouse embryo. *Development* **118**, 47-59.
Schubert, F. R., Fainsod, A., Gruenbaum, Y. and Gruss, P. (1995). Expression of the novel murine homeobox gene Sax-1 in the developing nervous system. *Mech. Dev.* **51**, 99-114.
Searcy, R. D., Vincent, E. B., Liberatore, C. M. and Yutzey, K. E. (1998). A GATA-dependent nkx-2.5 regulatory element activates early cardiac gene expression in transgenic mice. *Development* **125**, 4461-4470.
Sefton, M., Sánchez, S. and Nieto, M. A. (1998). Conserved and divergent roles for members of the Snail family of transcription factors in the chick and mouse embryo. *Development* **125**, 3111-3121.

Smyth, G. K. (2005). Limma: linear models for microarray data. In *Bioinformatics and Computational Biology Solutions Using R and Bioconductor* (ed. R. Gentleman, V. Carey, S. Dudoit, R. Irizarry and W. Huber), pp. 397-420. New York, NY: Springer.

Sumi, T., Oki, S., Kitajima, K. and Meno, C. (2013). Epiblast ground state is controlled by canonical Wnt/β-catenin signaling in the postimplantation mouse embryo and epiblast stem cells. *PLoS ONE* **8**, e63378.

Takada, S., Stark, K. L., Shea, M. J., Vassileva, G., McMahon, J. A. and McMahon, A. P. (1994). Wnt-3a regulates somite and tailbud formation in the mouse embryo. *Genes Dev.* **8**, 174-189.

Tam, P. P. and Behringer, R. R. (1997). Mouse gastrulation: the formation of a mammalian body plan. *Mech. Dev.* **68**, 3-25.

Teo, A. K., Arnold, S. J., Trotter, M. W., Brown, S., Ang, L. T., Chng, Z., Robertson, E. J., Dunn, N. R. and Vallier, L. (2011). Pluripotency factors regulate definitive endoderm specification through eomesodermin. *Genes Dev.* **25**, 238-250.

Tesar, P. J., Chenoweth, J. G., Brook, F. A., Davies, T. J., Evans, E. P., Mack, D. L., Gardner, R. L. and McKay, R. D. (2007). New cell lines from mouse epiblast share defining features with human embryonic stem cells. *Nature* **448**, 196-199.

Tzouanacou, E., Wegener, A., Wymeersch, F. J., Wilson, V. and Nicolas, J. F. (2009). Redefining the progression of lineage segregations during mammalian embryogenesis by clonal analysis. *Dev. Cell* **17**, 365-376.

Vallier, L., Mendjan, S., Brown, S., Chng, Z., Teo, A., Smithers, L. E., Trotter, M. W., Cho, C. H., Martinez, A., Rugg-Gunn, P. et al. (2009). Activin/Nodal signalling maintains pluripotency by controlling Nanog expression. *Development* **136**, 1339-1349.

Wilkinson, D. G., Bhatt, S. and Herrmann, B. G. (1990). Expression pattern of the mouse T gene and its role in mesoderm formation. *Nature* **343**, 657-659.

Wood, H. B. and Episkopou, V. (1999). Comparative expression of the mouse Sox1, Sox2 and Sox3 genes from pre-gastrulation to early somite stages. *Mech. Dev.* **86**, 197-201.

Yamaguchi, T. P., Takada, S., Yoshikawa, Y., Wu, N. and McMahon, A. P. (1999). T (Brachyury) is a direct target of Wnt3a during paraxial mesoderm specification. *Genes Dev.* **13**, 3185-3190.

Ying, Q. L., Stavridis, M., Griffiths, D., Li, M. and Smith, A. (2003). Conversion of embryonic stem cells into neuroectodermal precursors in adherent monoculture. *Nat. Biotechnol.* **21**, 183-186.